Ice Sheets, Oceans, and the Earth's Shape

W. R. PELTIER

Department of Physics, University of Toronto, Ontario, Canada

Abstract

A gravitationally self-consistent model has been constructed which predicts the history of relative sea level everywhere on the earth's surface subsequent to a major deglaciation event. The model has two unknown functionals which may be simultaneously constrained by comparing predictions of the model with observations. These functionals are: (1) the space and time dependent ice load on the surface, and (2) the radial variation of viscosity of the assumed linearly viscoelastic (Maxwell) earth. Here the theoretical structure of this model is reviewed and extensions are described to incorporate the influence of the lithosphere upon the relaxation spectrum. A limited number of comparisions between observed and predicted relative sea level are described and on the basis of the results obtained further extensions of the calculation are suggested.

1. Introduction

The response of the Earth and its oceans to massive continental deglaciation is controlled by two 'functionals' of the system, both of which are imperfectly known. These functionals, to which I have referred previously as M and V (Peltier, 1976), respectively describe the space and time-dependent surface mass load to which the planet is subject and the departure of its rheology from perfect Hookean elasticity. The former may be conveniently separated into two distinct parts as $M = M_I + M_o$ where M_I is the space dependent deglaciation chronology and M_o is the mass equivalent variation of bathymetry at each point in the ocean basins. If the hydrological cycle is closed then it is clear that M_I and M_o are not unrelated. In order to conserve mass during deglaciation the integral of M over the surface of the planet must vanish at all times. While the determination of M is normally considered to be the province of Quaternary geology, the estimation of the rheology functional V has been discussed most often in the geophysical literature.

The link between these two unknown quantities is sea level, or more precisely, the history of relative sea level at every point on the Earth's surface where ocean and land meet. Relative sea level is of course an 'observable'. Although the existence of this connection through the relative sea level data between the rheology of the interior of the Earth and its deglaciation chronology has long been appreciated, only recently has a theory been elaborated in terms of which the link is explicitly accounted for. In terms of this theory it has proven possible to reconcile a large fraction of the global data on relative sea level with a single deglaciation chronology and a single profile of mantle viscosity. Although the remaining misfits between theory and observation are large in some locations, most notably in the vicinity of the 'proglacial forebulge', agreement is sufficiently close that we may be justified in expecting that refinements of M and V will lead to accord within the observational uncertainty.

The detailed elaboration of this theory, which will be reviewed in a cursory fashion below, and accounts of its predictions are contained in a series of articles published in the past few years. Peltier (1974), extending earlier work by Farrell (1972) and Longman (1962) on elastic Earth models, invoked the 'Principle of Correspondence' to show how one could describe mathematically the response of a linearly viscoelastic (Maxwell) Earth to impulsive gravitational interaction with a point mass load. The Green functions for this problem were then employed by Peltier and Andrews (1976) to compute *approximate* relative sea level curves based upon the change in local radius and the neglect of ocean loading. In this paper the Green function for the perturbation in the gravitational potential was also deduced and a preliminary model of the deglaciation chronology constructed. Farrell and Clark (1976), using this deglaciation model and the gravitational potential Green function, showed how one could construct a self-consistent integral equation for relative sea level which satisfied the dual constraints of conservation of mass and the fact that the surface of the ocean must be an equipotential surface at all times. This made use of earlier work by Farrell (1973) on the elastic ocean tidal loading problem. Peltier (1976) considered the inverse problems of inferring M *and* V from the relative sea level data and suggested that the non-linear problem was amenable to attack using an iterative method. Finally, Clark, Farrell, and Peltier (1978) describe an extensive (although preliminary) series of comparisons between the predictions of theory and the observations. Further extensions of these calculations are suggested in the concluding section.

2. Theory

Here discussion will be confined to the theoretical structure of the forward problem of predicting the time-dependence of relative sea level given an accurate deglaciation chronology. No attempt will be made to describe the numerical methods employed to implement this theory. The interested reader is referred to the papers cited in the introduction for this information. In order to illustrate the theory and to extend it slightly I will consider Earth models which have rigid lithospheres at the surface and will compare the results to those which do not. One of the current debates concerning the anelasticity of the planetary interior, which the relative sea level data might be expected to resolve, is that concerning the thickness of this manifestation of the cold thermal boundary layer which forms the outer shell of the planet. The existence of this region inextricably couples the elastic and viscous components of the rheology and no previous spherical model has incorporated its effect. Furthermore the lithosphere introduces an additional time constant in the relaxation spectrum of every purely harmonic deformation of the surface, a time constant which differs from both those for the fundamental mantle and core modes (Peltier, 1976).

The Laplace transformed field equations for a self-gravitating viscoelastic Earth model in the quasi-static approximation (inertial force neglected) are

$$\underline{\nabla}\cdot\underline{\underline{\tilde{\tau}}} - \underline{\nabla}(\rho g \underline{\tilde{u}}\cdot\underline{e}_r) - \rho\nabla\tilde{\phi} + g\underline{\nabla}\cdot(\rho\underline{\tilde{u}})\underline{e}_r = 0, \tag{1a}$$

$$\nabla^2\tilde{\phi} = -4\pi G\underline{\nabla}\cdot(\rho\underline{\tilde{u}}), \tag{1b}$$

respectively the equation of momentum conservation and Poisson's equation for the perturbation $\tilde{\phi}$ of the ambient gravitational potential. The tilda represents implicit dependence upon the Laplace transform variable s, ρ is the density of the background hydrostatic equilibrium configuration, g the local gravitational acceleration, $\underline{\tilde{u}}$ the displacement field, and G the gravitational constant. $\underline{\underline{\tilde{\tau}}}$ is the Laplace transformed stress tensor, which for a Maxwell solid (Malvern, 1969) has the form

$$\tilde{\tau}_{ij} = \lambda(s)\tilde{e}_{kk}\delta_{ij} + 2\mu(s)\tilde{e}_{ij} \tag{2}$$

where
$$\lambda(s) = \frac{\lambda s + \mu K/\nu}{s + \mu/\nu} \tag{3a}$$

$$\mu(s) = \frac{\mu s}{s + \mu/v} \tag{3b}$$

$$K = \lambda + \frac{2}{3}\mu, \tag{3c}$$

and where λ and μ are the normal Lamé constants of elasticity. $\lambda(s)$ *and* $\mu(s)$ are compliances in terms of which the constitutive relation (2) between stress $\tilde{\tau}_{ij}$ and strain $\tilde{e}_{ij}$ has precisely the same *form* as that for a Hookean elastic solid. In (3a) and (3b) v is the equivalent Newtonian viscosity.

The mechanism by which the Maxwell solid responds to an applied stress may be readily understood by inspection of (3). Note that s and μ/v both have the dimensions of inverse time. We define a 'Maxwell time' T_m such that

$$T_m = v/\mu \tag{4}$$

For $s \gg T_m^{-1}$ (the short time limit) $\lambda(s) \to \lambda$ and $\mu(s) \to \mu$ and the material 'behaves' as a Hookean elastic solid. In the long time limit $(s \ll T_m^{-1})\lambda(s) \to K$, $\mu(s) = vs$ and the material behaves like a Newtonian viscous fluid with viscosity v. The material is viscously incompressible in the long time limit since $K = \lambda + \frac{2}{3}\mu$ is independent of s. These limiting behaviours are in accord with the conventional spring and dashpot in series analogy for a one dimensional Maxwell medium (Malvern, 1969).

To solve the surface loading problem for such an Earth model we invoke the 'Principle of Correspondence'. Operationally this amounts to little more than noting the analogy between (2) and the equivalent Hookean elastic form. We solve an 'equivalent' elastic problem for many values of the Laplace transform variable s and then simply invert the spectral solutions so obtained into the time domain. This equivalent elastic problem is the following. Assume that the Earth model is 'excited' by gravitational interaction with a point mass load of magnitude 1 kg which is brought to the surface from infinity at $t = 0$ and instantaneously removed. The solutions for the displacement field and for the gravitational potential perturbation may be expressed in series form as (with the tilda suppressed).

$$\underline{u} = \sum_{n=0}^{\infty} \left[U_n(r,s) P_n(\cos\theta)\hat{e}_r + V_n(r,s)\frac{\partial P_n(\cos\theta)}{\partial\theta}\hat{e}_\theta \right] \tag{5a}$$

$$\phi = \sum_{n=0}^{\infty} \Phi_n(r,s) P_n(\cos\theta) \tag{5b}$$

where $P_n(\cos\theta)$ is the usual Legendre polynomial of degree n, θ is the angular distance from the point of application of the load and the U_n, V_n, ϕ_n are spectral amplitudes. In analogy with the elastic problem these spectral amplitudes may be expressed in terms of a triplet of dimensionless scalar 'Love numbers' which are defined by

$$\begin{bmatrix} U_n(r,s) \\ V_n(r,s) \\ \Phi_{1,n}(r,s) \end{bmatrix} = \Phi_{2,n}(r) \begin{bmatrix} h_n(r,s)/g \\ l_n(r,s)/g \\ k_n(r,s) \end{bmatrix} \tag{6}$$

where the spectral amplitude Φ_n has been expanded as $\Phi_n = \Phi_{1,n} + \Phi_{2,n}$ where the $\Phi_{2,n}$ are the spherical harmonic coefficients of the expansion of the potential of the surface point mass load. The $\Phi_{2,n}$ are independent of s since the forcing is taken to be impulsive in the time domain.

Examples of the Love number s-spectra $h_n(a,s)$, where a is the radius of the Earth, are shown in Figs. 1 and 2 for two different viscoelastic Earth models. The elastic Lamé parameters and the density are the same for both models and are those for a standard Gutenberg–Bullen A Earth. The two models therefore differ only in their viscosity structure. In both models the core is assumed to be inviscid and the presence of the inner core is neglected. Fig. 1 shows Love number s-spectra for a model which has $v = 10^{22}$ P (cgs) throughout the mantle. It is the model which Cathles (1975), Peltier and Andrews (1976), and Clark, Farrell, and Peltier (1977) have suggested as providing a 'good' fit to the relative sea level data for a realistic deglaciation chronology. Evident in these spectra are the viscous (small s) and elastic (large s) asymptotes described above. However this model has no lithosphere and direct comparison of observation and theory shows that there are misfits

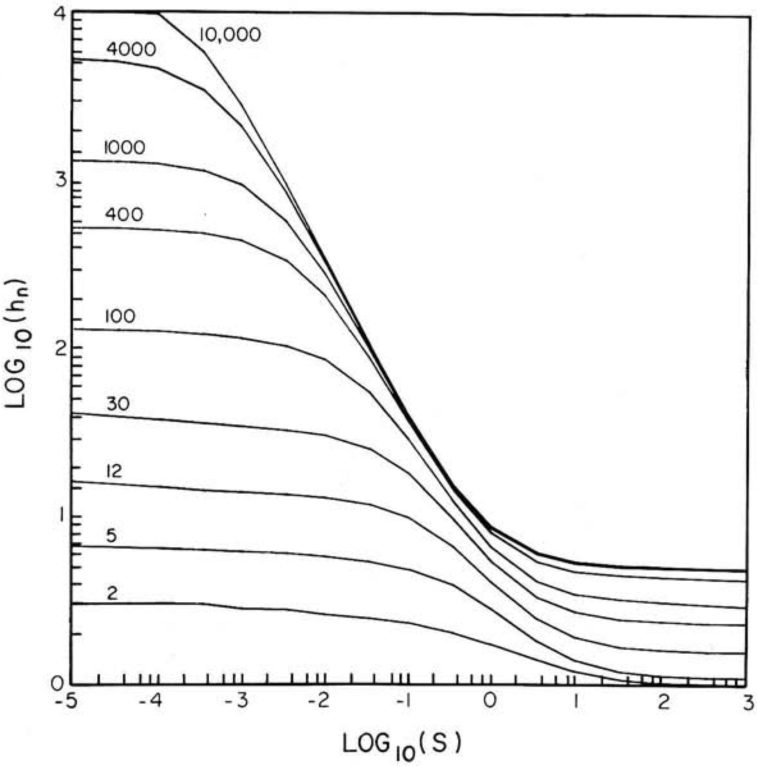

Fig. 1. Love number s-spectra $h_n(a,s)$ for the first Earth model described in the text. The model has $\nu = 0$ in the core and $\nu = 10^{22}$ P (cgs) throughout the mantle; it has no lithosphere. Note the large s (elastic) and small s (isostatic) asymptotes which exist for all n. The degree n of the Legendre harmonic is marked adjacent to each curve

in the vicinity of the peripheral bulge which may excede 100% in magnitude. This is precisely the region in which the influence of the lithosphere is expected to be most important. To remedy this defect we require an Earth model which contains this feature. Fig. 2 illustrates the effect upon the $h_n(a,s)$ spectra of a 'lithosphere' of thickness $T = 112.5$ km in which $\nu = \infty$. Here we have in fact plotted $h_n^v(a,s) = h_n(a,s) - h_n^E(a)$ where the $h_n^E(a)$ are the n-dependent elastic asymptotes. Comparison of Figs. 1 and 2 shows clearly that the main effect of the presence of the lithosphere is to entirely suppress the viscous relaxation of all sufficiently short wavelengths (sufficiently large n). In Fig. 2 $h_n^v(a,s) \equiv 0$ for $n \gtrsim 150$. This is entirely expected since short deformation wavelengths are not able to 'see through' the rigid lithosphere to the viscous region beneath and they are therefore supported elastically. This is not, however, the only effect of the lithosphere; it also modifies the relaxation *time spectra* substantially.

To see the way this works we invoke the normal mode expansion for the Love number s-spectra introduced by Peltier (1976) where it was shown that $h_n(a,s)$ and $k_n(a,s)$ could be exactly represented as, e.g.

$$h_n(a,s) = \sum_j \frac{r_j}{s + s_j} + h_n^E(a). \qquad (7)$$

Here the s_j determine a discrete set of relaxation times $\tau_j = s_j^{-1}$ which are associated with the relaxation of the harmonic deformation of degree n. These s_j are eigenvalues determined by solving the associated homogeneous boundary value problem and constitute a discrete set of poles on the negative real s-axis in the complex s-plane. The r_j are the residues

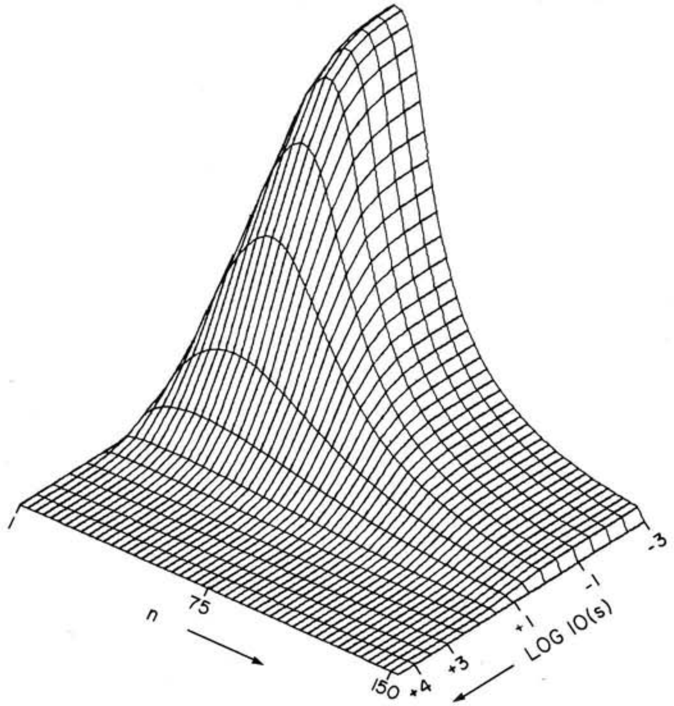

Fig. 2. A three dimensional view of the viscous part of the Love number s-spectra for the second viscosity model. This model differs from the first (Fig. 1) only in that it has a lithosphere of thickness $T = 112.5$ km in which $\nu = \infty$ at the surface. Note that for sufficiently large $n \gtrsim 150\, h_n^{\nu}(a,s) \equiv 0$ so that sufficiently short wavelengths are supported elastically

at the poles s_j for the inhomogeneous problem.

In Figs. 3 and 4 we show *relaxation diagrams* for the two viscosity modes described above. Inspection of these results indicates a strong dependence of the modal structure upon the lithosphere. When it is absent (Fig. 3) the relaxation spectrum is dominated by two main decay times, that for the fundamental mantle mode denoted by M0 and that for the core mode (C0). The shear energy in these modes is confined respectively to the earth's surface and to the core-mantle boundary (Peltier, 1976). The relaxation diagram for the model with lithosphere (Fig. 4) contains an additional mode (L0) in which the shear energy is confined to the vicinity of the base of the lithosphere. Neither M0 nor C0 are significantly effected by this feature for small n (large wavelength). Comparison of Fig. 2 and Fig. 4 shows that viscous relaxation is suppressed for values of n which exceed that for which M0 and L0 first become tangent. For all $n \gtrsim 30$ the decay time for M0 is reduced by the presence of the lithosphere and the extent of this reduction increases with n. This effect has been described previously by McConnell (1968) in the context of a study of non-gravitating half space models. It has not been described previously for the spherical self-gravitating models which are of interest to us here.

Further inspection of Figs. 3 and 4 shows that both models also support a family of modes which have exceptionally long relaxation times. These 'lower' modes are labelled M1, M2, ..., etc. in the figures and an analysis of the radial distribution of shear energy within them shows that the energy density peaks in the transition region of the mantle for small n (Peltier, 1976). The physical

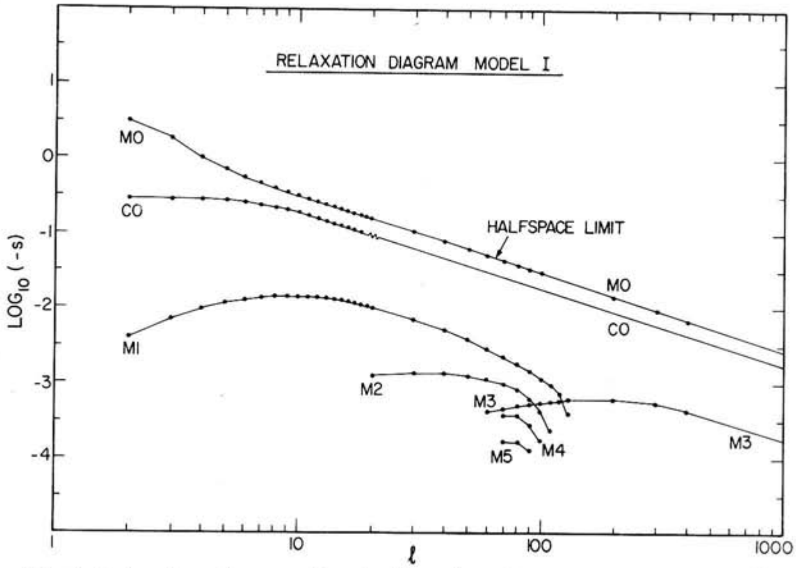

Fig. 3. Relaxation diagram for the first viscosity model where $\nu = 10^{22}$ P (cgs) throughout the mantle. The ordinate s is the inverse relaxation time and the time is non-dimensionalized with respect to the scale $[t] = 10^3$ years. Note that for large n the fundamental mantle mode (M0) is a straight line on this diagram as predicted by the uniform, non-gravitating half space model

mechanism which supports these modes is embodied in the fourth term on the left-hand side of the momentum balance equation (1a). From the linearized form of the equation of continuity $\underline{\nabla} \cdot (\rho \underline{u}) = -\rho'$, where ρ' is the perturbation density field; thus the fourth term is $-\tilde{\rho}/g\hat{e}_r$ which is just the Laplace transformed buoyancy force per unit volume.

Now in the elastic limit $t \ll T_m$ it is clear that this term must be retained; however in the viscous limit $t \gg T_m$ the retention of the buoyancy force in the linearized momentum balance equation involves an implicit assumption regarding the relation between the background density field $\rho(r)$ and that which would obtain if the radial variation of background temperature were adiabatic. To see this we may argue as follows. Neglecting isothermal compressibility the linearized form of the equation of state is just $\rho' = -\rho\alpha T'$ where α is the coefficient of thermal expansion. Furthermore the linearized and time integrated form of the equation of energy conservation for a fluid gives

$$T' \cong -u_r\left[\frac{dT}{dr} + \frac{\alpha T g}{c_p}\right]$$

Thus $\rho'\alpha u_r(dT/dr + \alpha Tg/c_p)$ and the term in brackets is the difference (since $dT/dr < 0$ and $T > 0$) between the actual and adiabatic temperature gradients. Thus if the background temperature field is everywhere adiabatic then $\rho' \equiv 0$ (regardless of the displacement field) and the fluid will feel no buoyancy force. This is an important point which requires an assumption to resolve. If we believe that the mantle is convectively 'mixed' then the effect of that mixing will be to establish a *nearly* adiabatic temperature profile (except perhaps through phase changes) in consequence of which the 'fast time scale' viscous gravitational relaxation will not be influenced by buoyancy. Here we have retained this contribution to the momentum balance and the result is the appearance of a family of modes with long decay times in the relaxation spectrum. In a a series of calculations which will be described elsewhere these effects have been analysed in detail. The existence of these modes does not, however, effect the performance of the model substantially since they are excited very inefficiently.

The Laplace inverse of s-spectra like (7) for either $h_n(s)$ or $k_n(s)$ is simply given by

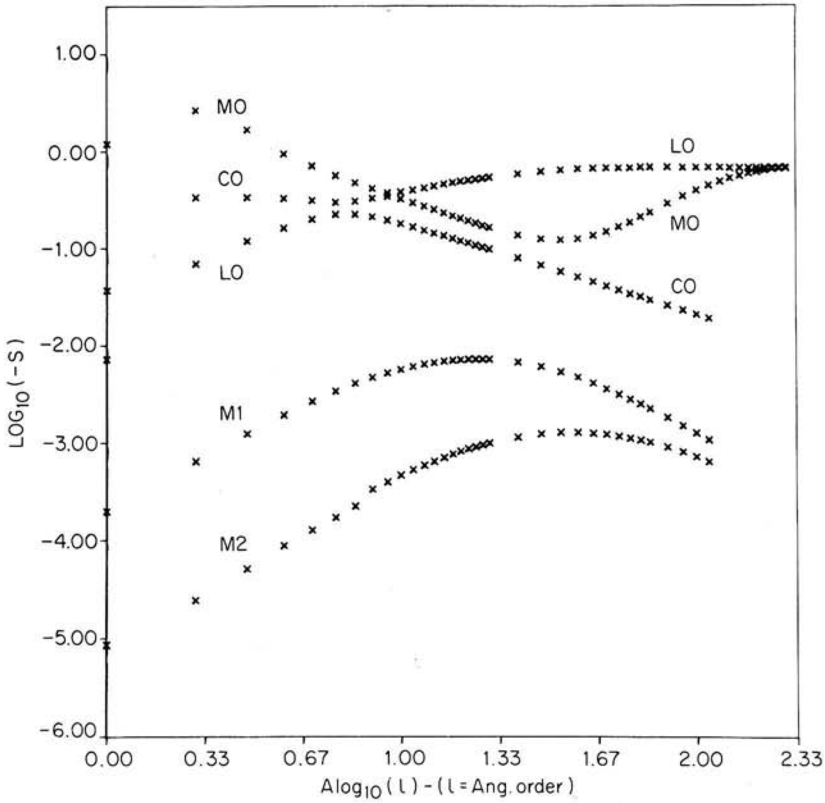

Fig. 4. Relaxation diagram for the second viscosity model which has a lithosphere of thickness $T = 112.5$ km in which $\nu = \infty$. Note that this relaxation diagram differs from that in Fig. 3 by the presence of an extra mode of relaxation (L0) which is entirely due to the presence of the lithosphere. In addition the fundamental mantle mode (M0) has decreased relaxation time for all $n \gtrsim 30$. The core mode (C0) is unaffected by the lithosphere

$$h_n(a,t) = \sum_j r_j e^{-s_j t} + h_n^E(a)\delta(t), \qquad (8)$$

and it should be recalled that this time domain response is that for an impulsive forcing. However this is not the response in which we are most interested. What we actually require is an expression for the spectral amplitudes of the solution in response to a point mass which is applied at $t = 0$ and allowed to remain on the surface for all subsequent times. We may obtain this from (8) simply by convolution with a Heaviside step function $H(t)$. The result is simply

$$h_n^H(a,t) = \sum_j \frac{r_j}{s_j}(1 - e^{-s_j t}) + h_n^E, \qquad (9)$$
$$= h_n^{H,v}(t) + h_n^E$$

and similarly for $k_n^H(a,t)$. These time domain forms are illustrated for the two viscosity models in Figs. 5 and 6 respectively. The most notable feature in these decay spectra which are plotted for $h_n^{H,v}(t)$ only is the striking difference in the amplitude of the response for $n > 30$ between the model with and without lithosphere. For $n \gtrsim 150$ the model with lithosphere (Fig. 6) shows *no* viscous relaxation. This was seen previously by direct inspection of the *s*-spectra.

In the limit $t \to \infty$ the planet and the point mass resting on its surface tend towards a new gravitational equilibrium configuration which is explicitly dependent upon the lithosphere thickness. This new isostatic state is one in which the spectral amplitudes have magnitude (Peltier, 1976).

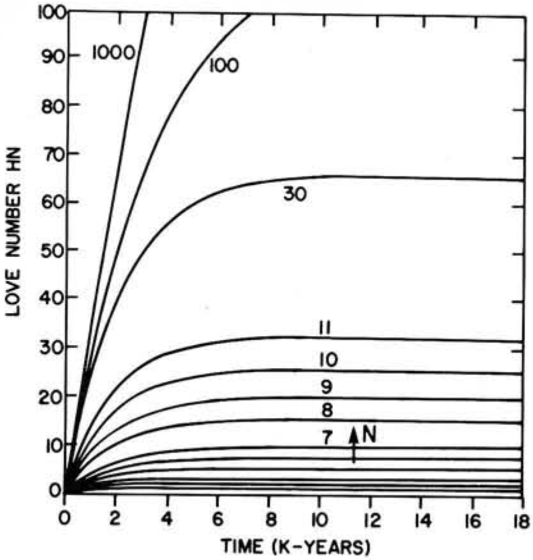

Fig. 5. Decay spectra $h_n^{H,v}(t)$ for the first viscosity model (no lithosphere). Note that the final amplitude of $h_n^{H,v}(t)$ is a continuously increasing function of n for this model. The value of n is marked on each curve and the time is shown in units of thousands of years

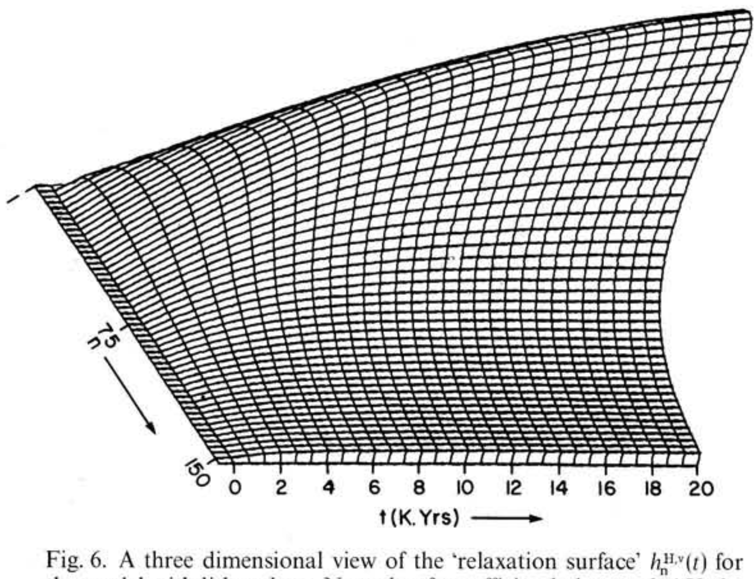

Fig. 6. A three dimensional view of the 'relaxation surface' $h_n^{H,v}(t)$ for the model with lithosphere. Note that for sufficiently large $n \gtrsim 150$ the amplitude of the harmonic of degree n shows no viscous relaxation. It is entirely supported elastically

$$\lim_{t\to\infty} h_n^H(a,t) = \sum_j \frac{r_j}{s_j} + h_n^E \qquad (10)$$
$$= \lim_{t\to 0} h_n(a,s)$$

as can be seen by direct inspection of (9) and (7). More formally we see that this is simply a consequence of the Final Value Theorem for Laplace transform pairs. From Fig. 1 or 5 it is clear that for the uniform v model the final amplitude (10) is infinite in the limit $n \to \infty$ and from Fig. 2 or 5 we see that this infinity is removed by the introduction of a lithosphere of finite (non-zero) thickness. Physically, this infinity is a simple consequence of the fact that a point mass resting on the surface of a *viscous* sphere will eventually sink to its centre since this is the only location at which it will feel no net force. When, as here, the lithosphere is treated as a shell with infinite viscosity this effect is prevented and all sufficiently short wavelengths are supported elastically. In the context of the present fully self-consistent viscoelastic model it is not necessary to specify separately a 'flexural parameter' for the lithosphere as has become common in the description of viscous half space models of the relaxation process. All of this information is contained *ab initio*.

In terms of the relaxation spectra $h_n^H(t)$ and $k_n^H(t)$ we may describe the process of isostatic equilibration in response to the point mass forcing in terms of any one of a number of signatures of the process. For example we might wish to know the time-dependent variation of the local radius or the variation in the vertical component of the gravitational acceleration or the variation of the gravitational potential on the deformed surface. These are the various *Green functions* of the process and they may be calculated by summing infinite series as described by Longman (1962) and Farrell (1972) for the elastic problem and by Peltier (1974) for viscoelastic models. Explicitly the expressions for the change in radius, the gravity anomaly, and the potential perturbation are respectively

$$U_r^H(a,\theta,t) = \frac{a}{M_e} \sum_{n=0}^{\infty} h_n^H P_n(\cos\theta) \qquad (11a)$$

$$g^H(a,\theta,t) = \frac{g}{M_e} \sum_{n=0}^{\infty} (n + 2h_n^H - (n+1)K_n^H) P_n(\cos\theta) \quad (11b)$$

$$\phi^H(a,\theta,t) = \frac{ag}{M_e} \sum_{n=0}^{\infty} (1 + k_n^H - h_n^H) P_n(\cos\theta) \qquad (11c)$$

where M_e is the mass of the Earth and where (11b) and (11c) describe the variations at a point on the deformed surface. The Green functions for radial displacement for the two viscosity models are shown in Figs. 7 and 8, respectively for the model without and with a lithosphere. Since the expressions (11) are infinite series it is clear from the previous discussion that the viscous parts will diverge at small θ as $t \to \infty$ in the model without lithosphere. This tendency is precisely that which is observed in Fig. 7. It is therefore not possible to *define* an 'isostatic' Green function when the lithosphere is absent. This is particularly important insofar as the comparison of predicted and observed gravity anomalies is concerned since the anomaly which we observe is really a measure of the degree of deviation from isostatic equilibrium. If the model cannot predict the final amplitude of the response then it certainly cannot predict the deviation from this final isostatic state which is recorded in the present day gravity anomalies.

Once the thickness of the lithosphere T is set then the isostatic asymptotes of the Love number s-spectra are fixed in turn and the isostatic Green functions are determined by summing along these small s asymptotes. The accuracy of the normal mode expansions for h_n and k_n may be checked in the isostatic limit by comparing the two expressions in (10). In Peltier (1976) the uniqueness of the state of isostatic equilibrium was invoked in the construction of a perturbation theory for the inference of mantle viscosity from the relative sea level data. This uniqueness exists only if the lithospheric thickness is not allowed to vary in the process of iterative improvement of the viscosity profile. Each time T is reset a new isostatic state results.

3. Implementation of the Theory

The Green functions in (11) are convenient summaries of the way in which a viscoelastic planet responds in the course of gravitational interaction with a point mass load on its surface. This interaction is the essence of glacial isostasy since the melting of glacial ice and the simultaneous filling of the ocean basins is a process which simply involves the *redistribution* of mass on the surface. *If* it were possible to observe directly, say, the time-dependence of the local radius of the planet at each point on its surface then one could construct a theory for the prediction of this observation simply by convolution of the

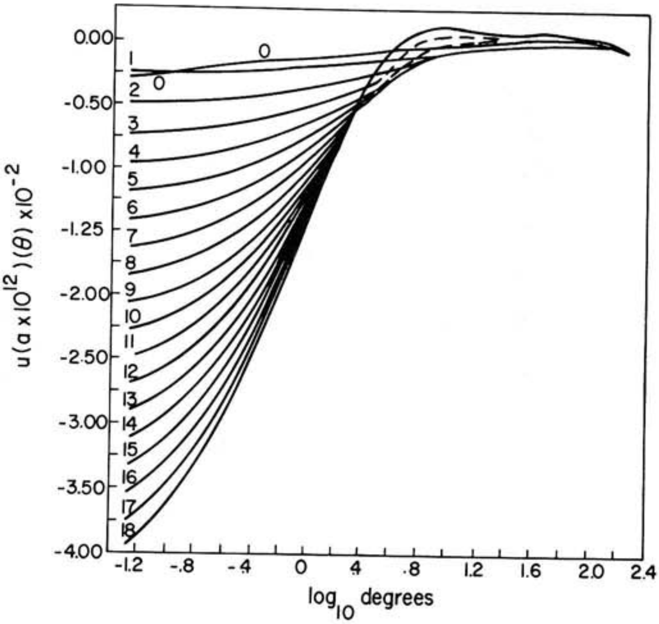

Fig. 7. Viscous part of the Green function for radial displacement $u_r^{H,v}$ defined in equation (11a) for the first viscosity model (without lithosphere). In this diagram the function has been normalized by multiplication by $(a\theta)$ to remove the effect of the geometric singularity as $\theta \to 0$. Note that in spite of this normalization the amplitude of the response continues to increase with increasing t and diverges as $t \to \infty$ (for small θ) as discussed in the text

Green function for radial displacement with the space and time-dependent surface load. This prediction would then take the form

$$\Delta R(\theta, \lambda, t) = \iint d\Omega' u_r^H(\theta - \theta', \lambda - \lambda'; t) M(\theta', \lambda') \tag{12}$$

where for simplicity it has been assumed (i) that the entire load redistribution takes place instantaneously at $t = 0$, and (ii) that prior to $t = 0$, the Earth and its ice sheets and oceans were in isostatic equilibrium. In (12) M has the dimensions of mass per unit area (density × thickness). The first assumption is obviously incorrect but it may be easily relaxed since a general history of load redistribution may be approximated to any accuracy by a series of discrete redistributions which are appropriately phased in time (see Peltier and Andrews, 1976).

We may test the second assumption directly by inquiring as to the time required to reach isostatic equilibrium after removal or application to the surface of a Laurentide or Fennoscandia size ice cap. If we consider a circular ice cap of radius $r_I = \underline{15}^\circ$, so that the forcing is approximately of Laurentide size, and use u_r^H for the viscoelastic model with lithosphere in (12) then the time-dependent response is that shown in Fig. 9. Inspection of this result illustrates two important points. Firstly, the relaxation time at the centre of the depression is strongly time-dependent with longer relaxation times becoming progressively more apparent as time proceeds. This is a direct consequence of the fact that in the spherical model each harmonic wavelength has a complete spectrum of relaxation times available to it as we have shown. The importance of each mode depends both upon the extent to which it is 'excited' by the point forcing (i.e. the r_j associated with each s_j at a particular n) and upon which n are promoted

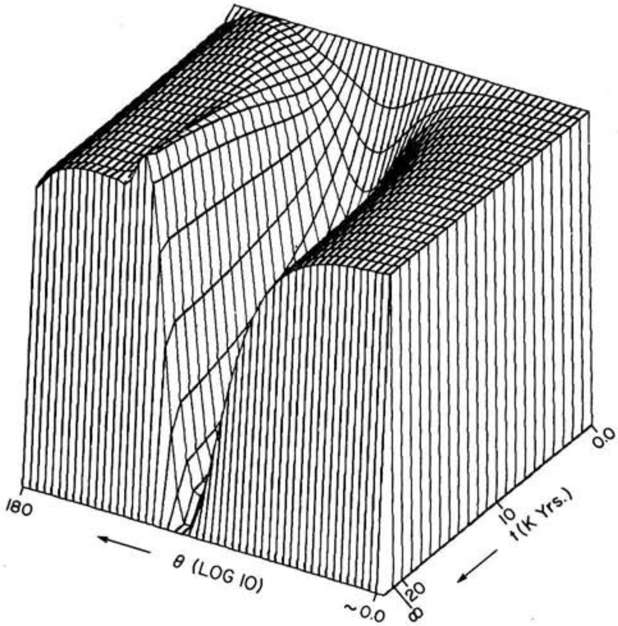

Fig. 8. A three dimensional view of the viscous part of the Green function for radial displacement $u_r^{H,v}$ for the viscoelastic model with lithosphere. As in Fig. 7 the function has been normalized by multiplication with $(a\theta)$ to remove the geometric singularity. Here the solution does not diverge at small θ and it is possible to calculate the isostatic Green function for the limiting time $t \to \infty$. This is marked explicitly on the figure

to dominance by a particular load history (spatial scale). The second point to note from Fig. 9 is the extremely long time required for the response to attain its full isostatic level in the central depression.

This long time scale for the late time interior response is a direct consequence of the existence of the higher modes due to buoyancy which have been retained in the models under discussion here. Models which support such higher modes have a 'long memory' of their past loading histories although their *initial* response to unloading is characterized by relatively short relaxation times. Such behaviour, and an understanding of those physical mechanisms through which it may be engendered, could be important for the reconciliation of rather large gravity anomalies with short observed relaxation times. Gravity anomalies 'see' the long time 'tail' of the relaxation curve whereas relative sea level is a memory of the initial response only.

Now equation (12) has been employed by Peltier and Andrews (1976) and its spectral equivalent by Cathles (1975) to calculate the *approximate* variations of relative sea level which are forced by a realistic deglaciation event (e.g. following the last glacial maximum). The use of (12) assumes in effect that the sea level variation is dominated by the variation of the radius of the solid earth and neglects the contribution to changes in sea level at the surface due to redistribution of mass in the interior. It also neglects the geoid variations which are effected by the self-gravitation of the oceans themselves. We may assess the validity of (12) only by doing a fully self-consistent calculation.

Before describing this calculation we first implement (12) and illustrate the extent to

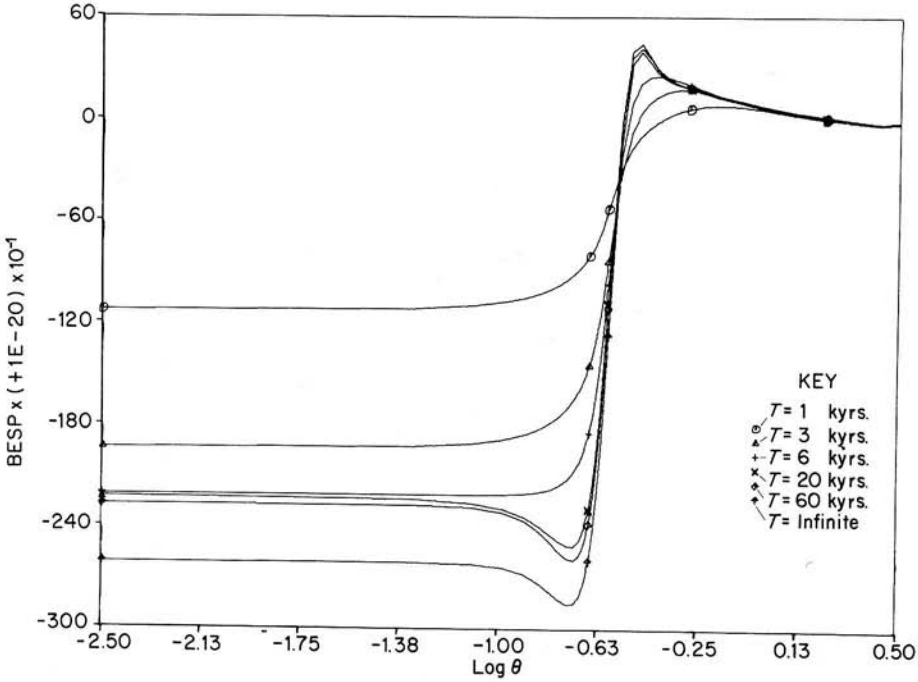

Fig. 9 The time-dependent variation of radius as a function of position (θ) produced by a disc load of radius $\theta_D = 15^\circ$ applied to the surface at $t = 0$ and maintained. The time in k years is marked adjacent to each curve. Note that the rate of relaxation in the central depression is strongly time-dependent with longer relaxation times dominating as time proceeds

which it is capable of providing accord with the observations. We require a model load history $M(\theta, \lambda, t)$ where in general $M = M_I + M_o$ as before. A discrete form of M_I has been tabulated by Peltier and Andrews (1976) from which may be deduced to model 'eustatic curve'. This is simply the mean increase in ocean depth as a function of time which, given $M_I(t)$ (assumed negative for load removal), may be calculated by assuming conservation of mass ($M_o = -M_I$), using the known area of the oceans and converting to a depth equivalent as

$$S_{EUS} = \frac{M_o(t)}{A_o \rho_w} \tag{13}$$

where A_o is the area of the ocean basins and ρ_w is the density of water. The model eustatic curve is compared in Fig. 10 with the 'observed' eustatic curve of Shephard (1963). The model deglaciation history is thus reasonable in this

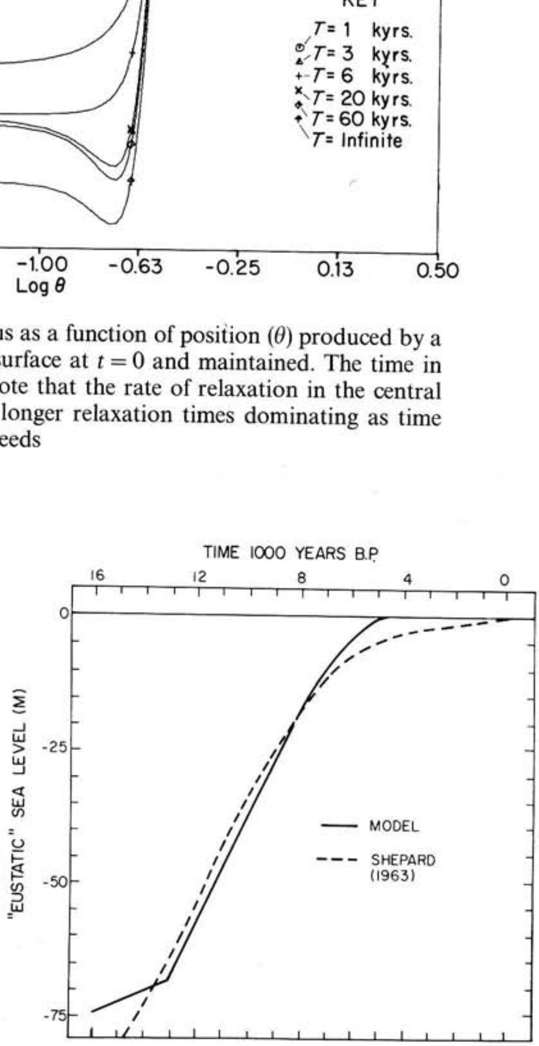

Fig. 10. Comparison of the model eustatic curve based upon the deglaciation chronology listed in Peltier and Andrews (1976) with the 'observed' eustatic curve of Shephard (1963). Note that in the model it is assumed that no changes in eustatic sea level occur after 5 k years BP

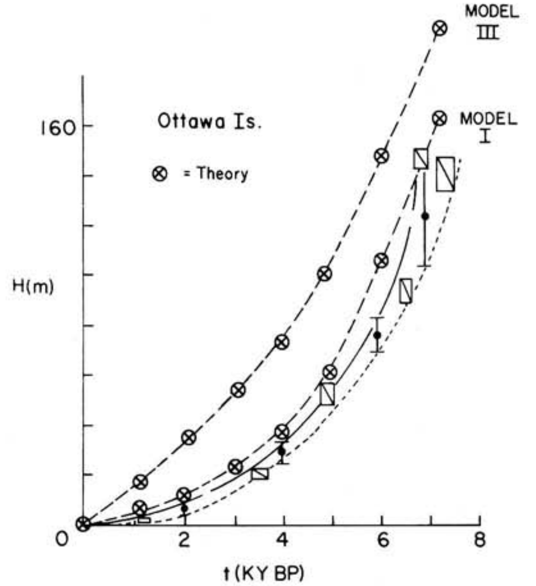

Fig. 11. Comparison of the approximate relative sea level prediction based upon equation (12) with the observed relative sea level data at the Ottawa Island site in Hudsons' Bay. The theoretical curve marked '1' is for the $\nu = 10^{22}$ P (cgs) uniform model. The curve marked '3' is for an Earth model which has a high viscosity lower mantle in which $\nu = 10^{24}$ P from a depth of 10^3 km to the core–mantle boundary

sense. Now equation (13) is really an integral constraint on the melting history and we do not wish to suggest by it that the meltwater added to the oceans leads to a uniform rise of bathymetry everywhere although this is the conventional assumption. Such a redistribution of mass to the oceans would lead to an ocean surface which was not a gravitational equipotential and the ocean would therefore not be in equilibrium. This is impossible. The question which we must answer given a model $M_I(\theta, \lambda, t)$ is 'How must the meltwater be distributed over the ocean basins such that the new ocean surface is indeed equipotential?'. Again, to answer this question requires the gravitationally self-consistent theory.

Initially we assume $M_o = 0$ so that the load redistribution M does not conserve mass. Inserting $M = M_I$ in (12) we do the convolution employing two Green functions u_r^H for models without lithospheres. The first of these has $\nu = 10^{22}$P everywhere and the second has $\nu = 10^{22}$P in the upper mantle and a lower mantle with $\nu = 10^{24}$P from a depth of 10^3 km to the core mantle boundary. In Figs. 11 and 12 we compare $\Delta R(\theta, \lambda, t)$ with the observed relative sea level curve at two sites. The first site is the Ottawa Islands site in Canada (Fig. 11) which is located near the centre of what was the Laurentide ice sheet and the second is for Florida on the southern tip of the eastern seaboard of the continental U.S. (Fig. 12). The agreement between the observations and the predictions of the $\nu = 10^{22}$P uniform model is excellent. The model with the high viscosity lower mantle is incompatible with the data. Such comparisons have led Cathles (1975) and Peltier and Andrews (1976) to suggest that rheological models which have rapidly increasing viscosity with depth are excluded by the rebound observations. If this suggestion is correct the consequences for mantle convection are important. Peltier (1972) has shown that if the mantle viscosity does not increase rapidly with depth then the radial 'mixing length' for convection should be on the order of the thickness of the mantle itself. If mantle wide convection is in fact the preferred mode of heat transport then it is possible to understand the large horizontal scales observed in the present day configuration of surface plates.

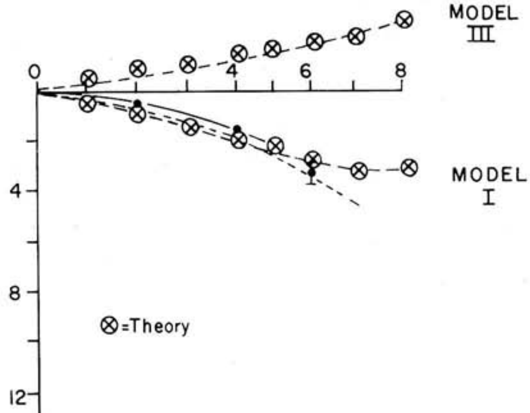

Fig. 12. Same as in Fig. 11 but for Florida. Notice that the model with high viscosity lower mantle predicts present day emergence whereas the observations and the $\nu = 10^{22}$ P uniform model indicate present day submergence

Because mantle rheology plays such an important role in geodynamic models of the long time scale convective processes we must question carefully the applicability of (12) which has been used to infer it from the rebound data. Firstly we must correct the predictions of (12) described above such that M is forced to conserve mass. If we make the correction by assuming $M_o(t)$ is uniformly distributed over the ocean basins, such as is conventional, then the corrections for $t \lesssim 5$ K years BP should be small in the 'near field' of the ice loads (Peltier and Andrews, 1976). However, such a correction is not gravitationally self-consistent as discussed above. What we require is a new theory for the prediction of relative sea level on a deglaciating Maxwell Earth which *is* self-consistent.

Such a theory has a particularly succinct and manageable form when it is constructed using the viscoelastic Green functions discussed in section 2. The function $\phi^H(a, \theta, t)$ defined in (11c) and calculated in Peltier and Andrews (1976) plays a fundamental role in the self-consistent model. That this turns out to be so should not be surprising since ϕ^H determines the perturbation in gravitational potential forced by the point load. Clearly the sea level variation must be intimately related to variations in potential since the surface of the oceans is constrained to be a gravitational *equipotential* at all points and for all time. The connection between ϕ^H and sea level $S(\theta, \lambda, t)$ on a deglaciating Earth has been described by Farrell and Clark (1976) following an earlier application of the same method by Farrell (1973) to a different problem. For a complete derivation the reader is referred to these articles. The gravitationally self-consistent equation for S is

$$S(\theta, \lambda, t) = \frac{\phi^H}{g} * M - \frac{M_I}{A_o \rho_w} - \left\langle \frac{\phi^H}{g} * M \right\rangle_o \tag{14}$$

where $\langle x \rangle_o$ denotes the average of the function x over the surface of the oceans, $*$ indicates convolution in space, and we have assumed a single instant of melting as before. Now (14) is an integral equation for S because M is S dependent. Indeed we express M in the form

$$M = \rho_I I + \rho_w S \tag{15}$$

where $I(\theta, \lambda, t)$ and $S(\theta, \lambda, t)$ are respectively the local variations of ice thickness and water thickness. Given ϕ^H for a particular rheological model and a deglaciation model $I(\theta, \lambda, t)$ equation (13) may be solved by relaxation to determine $S(\theta, \lambda, t)$. The S determined in this way actually describes the change in sea level with respect to a 'vertical metre stick' which is rigidly attached to the surface of the solid Earth. This is essentially due to the fact that ϕ^H defined in (11c) contains the Love number h_n^H and thus the potential perturbation includes a contribution from the local change in radius as well as the contribution (from k_n^H) due to the redistribution of mass in the interior. Averaging (13) over the oceans' surface we see that the conservation of mass constraint is also satisfied. When we predict sea level variations using (13) the prediction need not be corrected for the 'eustatic rise'. This is internally and consistently accounted for. Furthermore, from (13) the local rise in sea level will not be uniform over the ocean basins and the degree of non-uniformity is just that, by construction, which is required to ensure that the surface of the ocean remains a gravitational equipotential at all times. Clark, Farrell, and Peltier (1978) have described a complete set of sea level predictions using (13) and have compared these predictions with observations. These calculations were done using ϕ^H for the uniform viscosity model. Here, in Fig. 13 we illustrate this function for the model with lithosphere. In a later paper in this book Clark describes these calculations in detail. Here I will discuss a few examples from North America to illustrate the characteristic misfits which remain but before doing so I would like to demonstrate the extent to which predictions made using either (12) or (14) are compatible. This will enable us to understand the extent to which we should be prepared to accept the conclusion of Cathles (1975) and Peltier and Andrews (1976) vis-a-vis the viscosity of the mantle.

In the near field of a disintegrating ice sheet the ice forcing will dominate the water forcing since $\rho_I I \gg \rho_w S$ so that (14) is no

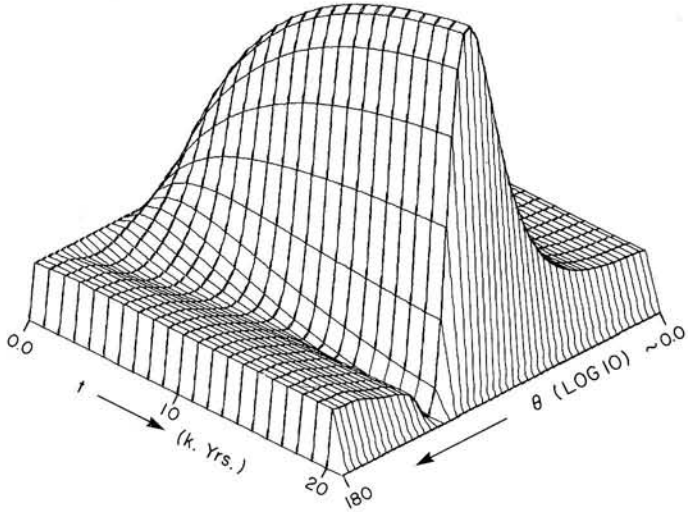

Fig. 13. Three dimensional view of the viscous part $\phi^{Hv}(\theta,t)$ of the Green function for gravitational potential perturbation for the model with lithosphere ($T = 112.5$ km). As in Figs. 7 and 8 the function has been normalized by multiplication with $(a\theta)$ to remove the effect of the geometric singularity at the origin $\theta = 0$

longer an integral equation, S appearing only on the left-hand side. Furthermore, for times sufficiently long after deglaciation is complete the last two terms will both be sensibly constant at a given site. These terms will therefore not contribute to further changes of sea level S. Subject to these two approximations (14) then becomes

$$S(\theta, \lambda, t) \cong \frac{\phi^H}{g} * \rho_I I - \text{Constant} \qquad (15)$$

and for comparison, (12) is of the form

$$\Delta R(\theta, \lambda, t) \cong u_r^H * \rho_I I \qquad (16)$$

The two predictions of sea level variations with respect to present day sea level at any fixed site therefore differ only as the functions ϕ^H/g and u_r^H. From (11) these are

$$\frac{\phi^H}{g} = \frac{a}{M_e} \sum_{n=0}^{\infty} (1 + k_n^H - h_n^H) P_n(\cos\theta) \qquad (17a)$$

$$u_r^H = \frac{a}{M_e} \sum_{n=0}^{\infty} h_n^H P_n(\cos\theta) \qquad (17b)$$

Now the first term in (17a) which represents the 'direct' contribution of the load to the potential fluctuation will lead only to an additional constant bias at each site since it is time-independent. If k_n^H were such that $k_n^H \ll h_n^H$ then (15) and (16) would lead to identical predictions. Equation (15) would predict a *fall of sea level* proportional to $-h_n^H$ and (16) would predict an uplift of the surface proportional to $+h_n^H$. The predictions would indeed be identical. The question then is whether the about inequality is in fact valid. Peltier (1974) has shown that the viscoelastic Love numbers are such that $nk_n^H \cong 0(h_n^H)$ for realistic Earth models, a result which is also true of their purely elastic counterparts (Farrell, 1972). Thus, for sufficiently small ice sheets spherical harmonic decompositions are dominated by large n, we may use (16) to predict relative sea level and expect that these predictions will be accurate in the near field. For large ice sheets, however, even in the near field and for times sufficiently long after melting (16) may be inaccurate and at least the simplified version of (14) (i.e. (15)) must be employed. From a more specific point of view what this means is that for $n \cong 5$ (the Laurentide ice sheet) (16) may be significantly in error whereas for $n \cong 16$ (the Fennoscandian ice sheet) (16) will be reasonably accurate. Of course (16) will not be

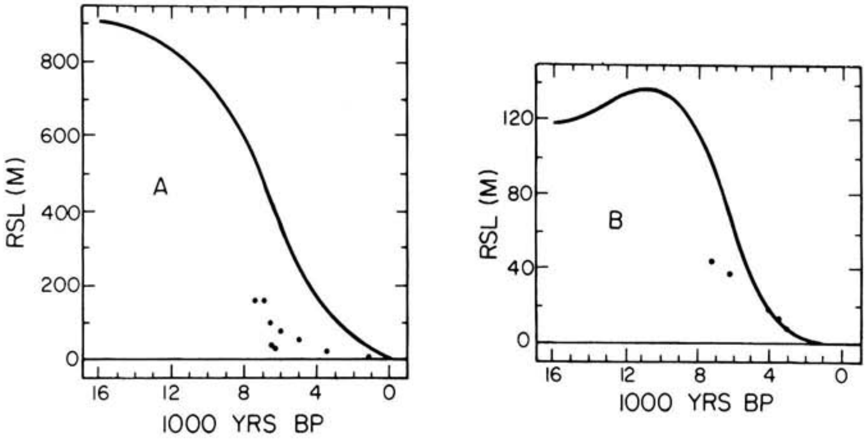

Fig. 14.(a) Computed and observed relative sea level for the Ottawa Islands, Hudson Bay, Canada (59.5°N, 80°W). The observations are the data of Andrews and Falconer (1969). The predicted emergence is considerably in excessed of the observations (see text for discussion). After Clark, Farrell, and Peltier (1978)

Fig. 14.(b) Computed and observed relative sea level for Inugsuin Fiord, Baffin Island, Canada (69.5°N, 70°W). The observations are those of Løken (1965). After Clark, Farrell, and Peltier (1978)

accurate even in the near field of the source for times which are within the period of active deglaciation and it will never be accurate in the far field where ocean loading effects are dominant.

The above analysis casts some doubt therefore upon the interpretations of mantle viscosity based upon (16) which have recently been presented by Cathles (1975) and by Peltier and Andrews (1976). In order to be sure of our interpretation we must employ the self-consistent model (14). Such a program has been undertaken in which the self-consistent sea level equation (14) coupled with the inverse theory described by Peltier (1976) are used to refine the viscosity model and the load history. This work will be described elsewhere when it has been completed. It *may* turn out as a result of these calculations that moderately high lower mantle viscosity will not be rejected by the gravitationally self-consistent model although I think it more likely that the original conclusion will be reinforced.

To illustrate the misfits which remain I will describe here a few of the results recently obtained by Clark, Farrell, and Peltier (1978) based upon the application of (14) for an Earth model in which $\nu = 10^{22}$P between the core-mantle boundary and the surface. In Fig. 14 are shown relative sea level curves for two sites: (14a) is for the Ottawa Islands, the same location for which the previous calculation (Fig. 11) was done using the Green function for radial displacement and neglecting ocean loading. The new calculation overestimates the total sea level fall for this particular site. It may be that the residual water load over Hudson Bay has been inadequately accounted for or that the lithosphere has a non-negligible influence even in the central depression. The same tendency is observed for Inugsuin Fjord on Baffin Island although here the agreement between observation and theory is much better, particularly in most recent times. Inspection of (14) or its simplified form (15) shows the errors between observed S and the prediction are as strongly coupled to errors in the load history as they are to errors in the viscosity model. However the load history which we employ (Peltier and Andrews, 1976) has a maximum thickness of 3.5 km over Hudsons Bay and if anything this may be a lower bound according to ice mechanical

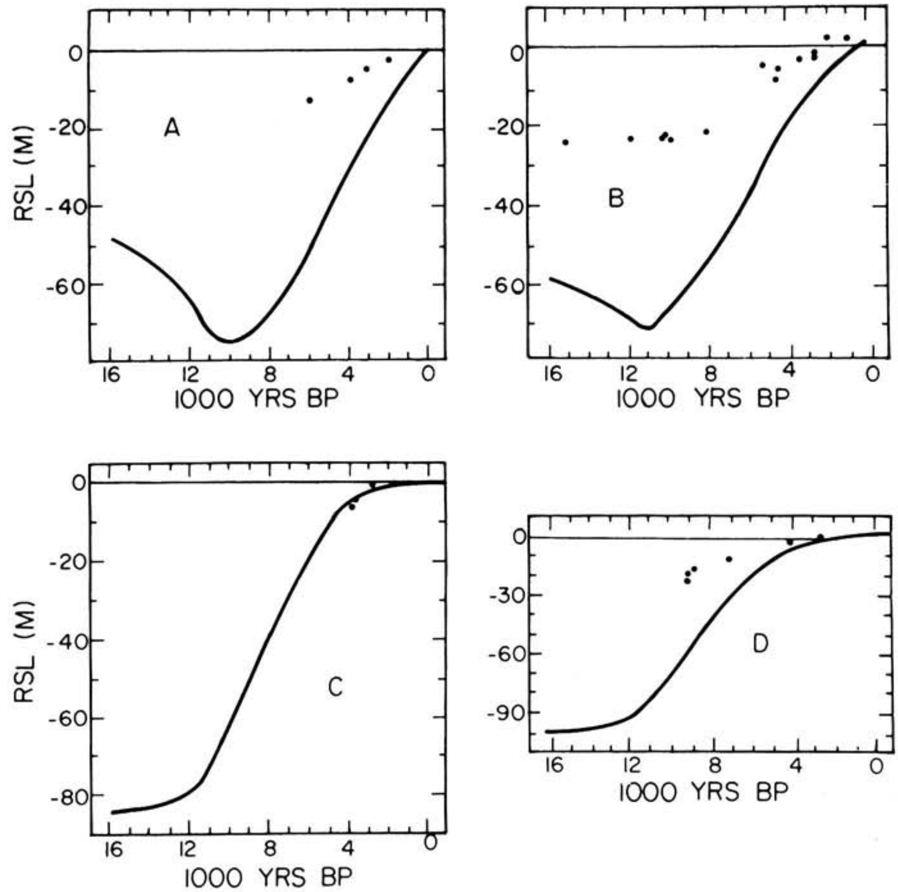

Fig. 15. Comparison of computed and observed relative sea level curves for a series of sites along the eastern seaboard of the USA. The locations and data sources are (a) Brigantine, New Jersey (39.4°N, 74.4°W): Stuiver and Daddario (1963); (b) Virginia (37.6°N, 75.7°W): Harrison and colleagues (1965) and Newman and Rusnak (1965); (c) Georgia (31°N, 81.4°W): Wait (1968); (d) Bermuda (32.3°N, 64.7°W): Neumann (1971). Note that for all these sites the predicted submergence is much greater than that observed. After Clark, Farrell, and Peltier (1978)

calculations, on the actual thickness which in fact existed. If we were to increase the ice thickness in the central dome the disagreement between theory and observation would be further magnified.

In Fig. 15 are shown the comparisons of observed relative sea level and the prediction for a sequence of sites located along the eastern seaboard of the U.S. The precise locations are described in the figure caption. In this region of submergence which is forced by the collapsing forebulge, although the qualitative form of the prediction (continuous submergence) is correct, the degree of submergence is considerably overestimated. There are misfits which are on the order of 100% of that which is observed.

If we consider sites which are located still further from the original location of the ice sheet the fit begins to improve considerably. In Figs. 16a and b are shown data for Florida and for the Gulf of Mexico respectively. Fig. 16a should be compared to the previous calculation (Fig. 12) which was done using the Green function for the variation of local radius and neglecting ocean loading. The self-consistent calculation gives a reasonably good fit but predicts a small amount of present day

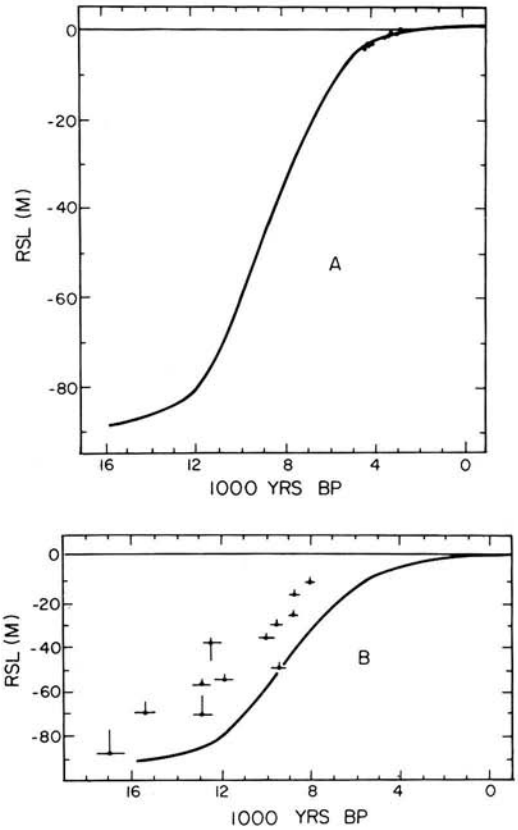

Fig. 16. Computed and observed relative sea level curves for (a) Florida (29° N, 84° W): Scholl and Stuiver (1967), and (b) Gulf of Mexico (27° N, 95° W): Curray (1960). After Clark, Farrell, and Peltier (1978)

emergence which is not observed. For the Gulf of Mexico (Fig. 16b), which has an extremely long record of relative sea level variation, the theory and observation are in rather close accord.

Given the above described discrepencies between theory and observation it is perhaps tempting to suggest that the deep mantle viscosity may be too low in the model. However, in the far field of the ice loads, where the self-consistent model is also valid, observation and theory are in agreement. Since the relaxation in the far field at mid oceanic sites is dominated by small n which 'see' the lower mantle rather clearly we are reluctant to abandon the 10^{22}P uniform model. The alternative explanation, that the misfits are due to the absence of a lithosphere in the model, is perhaps more attractive. Since the effect of the lithosphere is felt only in the near field and since this is where the largest misfits exist, it might be expected that the 'right' choice for the lithospheric thickness may lead to agreement with the data. A complete series of self-consistent calculations using the Green function described previously for a model with a lithospheric thickness of 112.5 km have recently been completed. Although this model gives a better fit to the data at the Ottawa Islands site in the central depression it does _not_ improve the fit in the vicinity of the peripheral bulge. On the basis of the good fit to the near field data in Fennoscandia (see Clark, this volume) we believe that the remaining misfits associated with the Laurentide recovery are due to an excessive load removal over Hudsons Bay (i.e. to errors in the local deglaciation chronology).

4. Conclusions

A complete and gravitationally self-consistent model for the prediction of variations of post-glacial sea level has been successfully constructed. The main physical assumption in the model is that the response of the Earth to mass loads applied to its surface is Newtonian. Our object in applying it is to test this hypothesis of Newtonian behaviour. We are not yet in a position to claim that it has been possible to find a single profile of the variation of viscosity with radius which reconciles theory and observation. Some of the misfits which remain may be due, in fact are surely due, to errors in our assumed deglaciation history. Also, and as we have suggested implicitly above, some of these errors may be due to the assumption that 20,000 years ago at glacial maximum the Earth and its ice sheets and oceans were in isostatic equilibrium. The process of disentangling these various effects will require a good deal of further calculation.

Here we have extended the theory slightly by determining the required Green functions for Earth models which have a rigid lithosphere at the surface and discussing their properties. The effect of the lithosphere has not been previously incorporated in any spherical model of the isostatic adjustment process. If one is interested in calculating the final isostatic response to a given applied load then it is mandatory that this region be included in the model. The lithospheric thickness (if the region is treated as perfectly elastic) determines the extent to which each harmonic constituent in the deformation is supported elastically. Since observed gravity anomalies are explicitly related to the *departure* from equilibrium, and since lithospheric thickness strongly modulates the final amplitude of the viscous relaxation, thus the computation of gravity anomalies requires the use of a model with lithosphere. In future calculations the observed gravity anomalies will be incorporated as further constraints on the model.

An additional effect which we are now preparing to explore is the extent to which the rotation of the Earth itself is affected by the deglaciation process. The redistribution of surface mass produces relatively large changes in the components of the inertia tensor and as the shape of the Earth relaxes following deglaciation a continuous change in the rate of rotation (length of the day) will result. Using the variation in surface load computed from the gravitationally self-consistent model we will be able to calculate this effect rather accurately and to compare it to the astronomical data.

References

Andrews, J. T. and Falconer, G., 1969. 'Late Glacial and Post Glacial history and emergence of the Ottawa Islands, Hudson Bay, N.W.T.', *Can. J. Earth Sci.*, **6**, 1263.

Cathles, L. M., 1975. *The Viscosity of the Earths Mantle*, Princeton University Press, New Jersey, U.S.A.

Clark, J. A., Farrell, W. E. and Peltier, W. R., 1978. 'Global changes of post glacial sea level: a numerical calculation', *Quaternary Res.*, **9**, 265–287.

Curray, J. R., 1960. 'Sediments and history of holocene transgression, continental shelf, northwest Gulf of Mexico', in 'Recent Sediments N. W. Gulf of Mexico', *Amer. Assoc. Petrol. Geol.*, 221.

Farrell, W. E., 1972. 'Deformation of the earth by surface loads', *Rev. Geophys. Space Phys.*, **10**, 761.

Farrell, W. E., 1973. 'Earth tides, ocean tides, and tidal loading', *Phil. Trans. R. Soc. London*, **A 274**, 45.

Farrell, W. E. and Clark, J. A., 1976. 'On postglacial sea level', *Geophys. J. R. astr. Soc.*, **46**,647.

Harrison, W., Malloy, R. J., Pusmak, G. A. and Terasmse, J., 1965. 'Possible late Pleistocene uplift Chesapeake Bay Entrance', *J. Glaciology*, **73**, 201.

Løken, O. H., 1965. 'Postglacial convergence at the south end of Inugsuin Fiord, Baffin Island, N.W.T.', *Geogr. Bull.*, **1**, 243.

Longman, I. M., 1962. 'A Green's function for determining the deformation of the earth under surface mass loads, 1, Theory', *J. Geophys. Res.*, **67**, 845.

Malvern, L. E., 1969. *Introduction to the Mechanics of a Continuous Medium*, Prentice-Hall, Inc., Englewood Cliffs, New Jersey.

McConnell, R. K., 1968. 'Viscosity of the mantle from relaxation time spectra of isostatic adjustment', *J. Geophys. Res.*, **73**, 7089.

Neumann, C. A., 1971. 'Quaternary sea-level data from Bermuda', *Quaternaria*, **14**, 41.

Newman, W. S. and Rusnak, G. A., 1965. 'Holocene submergence of the eastern shore of Virginia', *Science*, **148**, 1464.

Peltier, W. R., 1972. 'Penetrative convection in the planetary mantle', *Geophys. Fluid Dyn.*, **3**, 265.

Peltier, W. R., 1974. 'The impulse response of a Maxwell Earth', *Rev. Geophys. Space Phys.*, **12**, 649.

Peltier, W. R., 1976. 'Glacial–isostatic adjustment—II. The inverse problem', *Geophys. J. R. astr. Soc.*, **46**, 669.

Peltier, W. R. and Andrews, J. T., 1976. 'Glacial–isostatic adjustment—I. The forward problem', *Geophys. J. R. astr. Soc.*, **46**, 605.

Scholl, D. W. and Stuiver, M., 1967. 'Recent submergence of southern Florida: a comparison with adjacent coasts and other eustatic data', *Geol. Soc. Amer. Bull.*, **78**, 437.

Shepard, F. P., 1963. '35,000 years of sea level', in *Essays in Marine Geology*, Univ. Southern California Press, 1.

Stuiver, M. and Daddario, H. J., 1963. 'Submergence of the New Jersey coast', *Science*, **142**, 951.

Wait, R. L., 1972. 'Submergence along the Atlantic coast of Georgia', *U.S.G.S. Prof. Paper*, **600–D**, 38.